Park, B. K. *J. Korean Chem. Soc.* **1993**, *37*, 431. (b) Doh, M. K.; Kim, B. G.; Jung, M. J.; Song, Y. D.; Park, B. K. *J. Korean Chem. Soc.* **1993**, *37*, 903. (c) Kim, B. G.; Yang, K.; Jung, M. J.; Doh, M. K. *J. Korean Chem. Soc.* **1994**, *38*, 456.
11. Shriver, D. F.; Drezdzon, M. A. *The Manipulation of Air-sensitive Compounds*; John Wiley & Sons: U. S. A., 1986.
12. Doyle, J. R.; Slade, P. E.; Jonassen, H. B. *Inorg. Synth.* **1960**, *6*, 216.
13. Frisch, M. J.; Trucks, G. W.; Schlegel, H. B.; Gill, P. M. W.; Johnson, B. G.; Robb, M. A.; Cheeseman, J. R.; Keith, T.; Peterson, G. A.; Montgomery, J. A.; Raghavachari, K.; Al-Laham, M. A.; Zakrzewski, V. G.; Ortiz, J. V.; Foresman, J. B.; Cioslowski, J.; Stefanov, B. B.; Nanayakkara, A.; Challacombe, M.; Peng, C. Y.; Ayala, P. Y.; Chen, W.; Wong, M. W.; Andres, J. L.; Replogle, E. S.; Comperts, R.; Martin, R. L.; Fox, D. J.; Binkley, J. S.; DeFrees, D. J.; Baker, J.; Stewart, J. J. P.; Head-Gordon, M.; Gonzalez, C.; Pople, J. A. Gaussian 94, Gaussian Inc.; Pittsburgh, PA, 1995.
14. (a) Hay, P. J.; Wadt, W. R. *J. Chem. Phys.* **1985**, *82*, 270. (b) Wadt, W. R.; Hay, P. J. *J. Chem. Phys.* **1985**, *82*, 284.
15. Hanack, M. *Conformational Theory*; Academic Press: U. S. A. 1965; pp 158-162.
16. Camalli, M.; Caruso, F.; Chaloupka, S.; Leber, E. M.; Rimml, H.; Venanzi, L. M. *Helv. Chim. Acta* **1990**, *73*, 2263.
17. (a) Steffen, W. L.; Palenik, G. J. *Inorg. Chem.* **1976**, *10*, 2432. (b) Stang, P. J.; Cao, D. H.; Poulter, G. T.; Arif, A. M. *Organometallics* **1995**, *14*, 1110. (c) Onuma, K.; Nakamura, A. *Bull. Chem. Soc. Jpn.* **1981**, *54*, 761.

A New Functional Model of Catechol Dioxygenases: Properties and Reactivity of [Fe(BLPA)DBC]BPh_4

Ji H. Lim, Ho J. Lee, Kang-Bong Lee†, and Ho G. Jang*

Department of Chemistry, Korea University, Seoul 136-701, Korea
†Advanced Analysis Center, KIST, Seoul 136-130, Korea
Received July 15, 1997

[Fe^{III}(BLPA)DBC]BPh_4, a new functional model for the catechol dioxygenases, has been synthesized, where BLPA is bis((6-methyl-2-pyridyl)methyl)(2-pyridylmethyl)amine and DBC is 3,5-di-*tert*-butylcatecholate dianion. The BLPA complex has a structural feature that iron center has a six-coordinate geometry with N_4O_2 donor set. It exhibits EPR signals at g=5.5 and 8.0 which are typical values for the high-spin Fe^{III} (S=5/2) complex with axial symmetry. The BLPA complex reacts with O_2 within a few hours to afford intradiol cleavage (75%) and extradiol cleavage (15%) products which is very unique result of all [Fe(L)DBC] complexes studied. The iron-catecholate interaction of BLPA complex is significantly stronger, resulting in the enhanced covalency of the metal-catecholate bonds and low energy catecholate to Fe^{III} charge transfer bands at 583 and 962 nm in CH_3CN. The enhanced covalency is also reflected by the isotropic shifts exhibited by the DBC protons, which indicate increased semiquinone character. The greater semiquinone character in the BLPA complex correlates well with its high reactivity towards O_2. Kinetic studies of the reaction of the BLPA complex with 1 atm O_2 in CH_3OH and CH_2Cl_2 under pseudo-first order conditions show that the BLPA complex reacts with O_2 much slower than the TPA complex, where TPA is tris(2-pyridylmethyl)amine. It is presumably due to the steric effect of the methyl substituent on the pyridine ring. Nevertheless, both the high specificity and the fast kinetics can be rationalized on the basis of its low energy catecholate to Fe^{III} charge transfer bands and large isotropic NMR shifts for the BLPA protons. These results provide insight into the nature of the oxygenation mechanism of the catechol dioxygenases.

Introduction

The catechol dioxygenases are non-heme iron enzymes that catalyze the oxidative cleavage of catechols and serve as part of nature's strategy for degrading aromatic molecules in the environment.[1] They are found in soil bacteria with two different types: one is intradiol-cleaving enzymes utilize Fe(III), and the other is extradiol-cleaving enzymes utilize Fe(II) and Mn(II). Significant progress[2-7] has been made in understanding the active site of the intradiol cleaving enzymes and is highlighted by the recent solution of the crystal structure of native protocatechuate 3,4-dioxygenase(3,4-PCD) showing that the iron(III) center of the active site of 3,4-PCD enzyme has five-coordinate geometry.[8] Furthermore, many spectroscopic studies suggested that the iron(III) center remains as a five-coordinate system even after binding with substrate catechol.[9,10] Model systems that mimic enzyme reactions are important mechanistic tools, because the flexibility in ligand design allows a systematic investigation of the important factors affecting reactivity as well as reac-

tion mechanism.[11-16]

In the previous biomimetic efforts, many scientists have focused on obtaining structurally characterized complexes capable of oxidative cleavage activity.[12-16] By studying a series of [Fe^{III}(L)DBC] complexes where L is a tetradentate tripodal ligand,[17] Que and coworkers have demonstrated a direct correlation between the rate of oxidative cleavage of the bound catecholate ligand and the Lewis acidity of the ferric center, the rate determining step involving the attack of dioxygen on the complex.[12-15] It was proposed that the increased Lewis acidity of the ferric center enhances the covalency of the metal-catecholate interaction and the semiquinone character of the bound catecholate, thereby activating the catecholate for reaction with O_2.[14,15]

These observations provide the rationale for the proposed substrate activation mechanism.[18] In this mechanism (Scheme 1), the substrate catecholate becomes activated upon coordination to the iron due to the ligand-to-metal charge transfer and reacts with dioxygen to yield a peroxide intermediate. This intermediate then decomposes to organic products.

In this paper, we report the spectroscopic and kinetic properties of [Fe(BLPA)DBC]BPh_4, thus far having the iron center of the greatest Lewis acidity in the [Fe(L)DBC] series. We discuss the arguments for the role of the metal center in the substrate activation mechanism proposed for the dioxygenases.

Experimental Section

All reagents and solvents were purchased from commercial sources and used as received, unless noted otherwise. Acetonitrile was distilled from CaH_2 under nitrogen before use. $DBCH_2$ was purified by recrystallization from hexane. $DBCH_2$-4,6-d_2 was prepared by deuterium exchange in D_2O in the presence of a substoichiometric amount of base at 140 °C in a sealed tube for ~4 hours.[19] Microanalyses were performed by Basic Science Research Center, Seoul.

Synthesis of bis((6-methyl-2-pyridyl)methyl)(2-pyridylmethyl)amine, BLPA. 1.28 g (10 mmole) 2-pyridylmethyl chloride was added slowly to 2.27 g (10 mmole) bis(6-methyl-2-pyridylmethyl)amine in 100 mL ethanol which was prepared according to the published procedure.[20] The reaction mixture was refluxed for 8 hours and concentrated under reduced pressure. The residue was dissolved in 30 mL dichloromethane and washed with water three times and then dried over anhydrous $MgSO_4$. The product was purified by chromatography employing the eluent (ethylacetate : ethanol=2 : 1) to afford a colorless solid (75% yield).

mp 84-85 °C, ^{1}H NMR ($CDCl_3$): δ 2.52 (s, Lu-CH_3), 3.85 (s, Lu-CH_2-), 3.88 (s, Py-CH_2-), 6.9 (d, Lu-β'), 7.1 (t, Py-β'), 7.45 (d, Lu-β), 7.57 (t, Lu-γ), 7.65 (q, Py β, γ), 8.5 (d, Py-α').

Synthesis of [Fe(BLPA)DBC]BPh_4. [Fe(BLPA)DBC]BPh_4 was synthesized by reacting 153.5 mg (0.38 mmol) $Fe(NO_3)_3 \cdot 9H_2O$ and 120.8 mg (0.38 mmol) BLPA in 20 mL ethanol under argon and adding 84.5 mg (0.38 mmol) $DBCH_2$ in 4 mL ethanol under argon after 30 min, followed by the slow addition of 2 equivalent triethylamine. The resulting dark purple-blue solution was treated with 130 mg (0.38 mmol) $NaBPh_4$, causing the immediate precipitation of a purple-blue powder, which was dried under vacuum (73% yield). Complex was purified by vapor diffusion of ether into an acetonitrile solution of crude product.

FAB-Mass m/z 594. Anal. Calcd. for [Fe(BLPA)DBC]BPh_4, $C_{58}H_{61}BFeN_5O_2$: C, 75.16; H, 6.63; N, 7.56. Found: C, 75.26; H, 6.75; N, 7.51.

Characterization of Oxygenation Products. The four major and one minor organic products of the [Fe(BLPA)DBC]$^+$ oxygenation reaction were identified by using GC, GC-Mass, HPLC, IR, and NMR spectroscopy. Spectroscopic data are as follows:

3,5-di-*tert*-butyl-5-(carboxymethyl)-2-furanone: IR (KBr) υ_{CO} 1755, 1723 cm^{-1}, $\upsilon_{C=C}$ 1644 cm^{-1}; ^{1}H NMR ($CDCl_3$): δ 0.96 (s, 9H), 1.21 (s, 9H), [2.74, 2.81, 2.91, 2.98 (AB q, J_{AB}=14 Hz, 2H)], 6.93 (s, 1H), 9.70 (s); ^{13}C NMR ($CDCl_3$): δ 24.9 (q), 27.6 (q), 31.2 (s), 37.1 (t), 37.4 (s), 87.8 (s), 143.6 (s), 145.2 (d), 170.9 (s), 174.7 (s).

3,5-di-*tert*-butyl-1-oxacyclohepta-3,5-diene-2,7-dione: IR (KBr) υ_{CO} 1783, 1741 cm^{-1}, $\upsilon_{C=C}$ 1636, 1600 cm^{-1}; ^{1}H NMR ($CDCl_3$): δ 1.16 (s, 9H), 1.28 (s, 9H), 6.14 (d, J=2 Hz, 1H), 6.45 (d, J=2 Hz, 1H); ^{13}C NMR ($CDCl_3$): δ 28.4 (q), 28.9 (q), 36.2 (s), 36.5 (s), 115.5 (d), 123.9 (d), 148.0 (s), 160.0 (s), 162 (s).

3,5-di-*tert*-butyl-2-pyrone: IR (KBr) υ_{CO} 1710 cm^{-1}, $\upsilon_{C=C}$ 1635, 1560 cm^{-1}; ^{1}H NMR ($CDCl_3$): δ 1.20 (s, 9H), 1.32 (s, 9H), 7.04 (d, 1H), 7.14 (d, 1H); ^{13}C NMR ($CDCl_3$): δ 28.4 (q), 29.5 (q), 31.9 (s), 34.8 (s), 127.4 (s), 136.2 (s), 136.3 (s), 143.8 (d), 160.9 (s).

4,6-di-*tert*-butyl-2-pyrone: IR (KBr) υ_{CO} 1710 cm^{-1}, $\upsilon_{C=C}$ 1630, 1550 cm^{-1}; ^{1}H NMR ($CDCl_3$): δ 1.19 (s, 9H), 1.26 (s, 9H), 6.01 (d, 2H); ^{13}C NMR ($CDCl_3$): δ 28.1 (q), 29.0 (q), 35.5 (s), 36.2 (s), 98.7 (s), 107.2 (s), 163.4 (d), 167.7 (d), 171.4 (s).

3,5-di-*tert*-butyl-5-(formyl)-2-furanone: IR (KBr) υ_{CO} 1756, 1744, 1725 cm^{-1}; ^{1}H NMR ($CDCl_3$): δ 1.05 (s, 9H), 1.25 (s, 9H), 6.90 (s, 1H), 9.60 (s, 1H); ^{13}C NMR ($CDCl_3$): δ 24.8 (q), 28.1 (q), 32.2 (s), 38.5 (s), 94.5 (s), 141.3 (d), 146.1 (s), 170.5 (s), 197.3 (d).

Physical Methods. UV-visible spectra were obtained

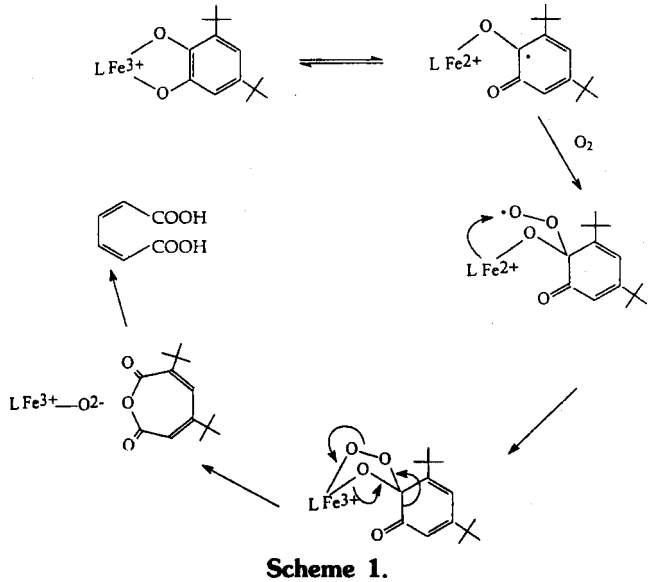

Scheme 1.

on a Hewlett-Packard 8452A diode array spectrophotometer and the near-IR region was recorded with a Hewlett-Packard 8453 biochemical analysis spectrophotometer. IR spectra were obtained Bomem 102 FT-IR spectrometer. Standard organic product analyses were performed using a Hewlett-Packard 5890 Series II Gas Chromatograph equipped with a flame ionization detector or a reverse-phase isocractic HPLC (Orom Vintage 2000 high performance liquid chromatography; with a variable wavelength detector. Reaction mixtures were separated by using C18 column). ^{1}H NMR spectra were obtained on a Varian VXR 300 and VXR 600 spectrometer. An inversion-recovery pulse sequence (180°-t-90°-ACQ) was used to obtain non-selective proton longitudinal relaxation times (T_1) with carrier frequency set at several different positions to ensure the validity of the measurements.

Oxygenation studies. Reactivity studies were performed in organic solvents in an oxygen atmosphere under ambient conditions. After the reaction was complete, as indicated by the loss of color, the solution was concentrated under reduced pressure. The organic products were extracted with ether, dried over anhydrous Na_2SO_4, and then concentrated. The remaining residue was dissolved in CH_3CN and acidified with HCl to pH 3 to decompose the dinuclear Fe^{III}BLPA complex. The furanone acid was extracted with ether, dried, and concentrated. The extracts were then subjected to GC or reverse-phase isocractic HPLC separation (conditions are same as previously reported in reference 14).

Kinetic studies were performed on an HP-8452A diode array spectrometer with temperature control by an Endocal RTE-5 refrigerated circulation bath. Oxygen was bubbled through the solution (0.5-0.8 mM in complex) and then maintained at 1 atm of pressure above the reacting solution. The oxygenation kinetics was followed by monitoring the disappearance of the low energy catecholate to FeIII charge transfer band of the BLPA complex.

Results and Discussion

Spectroscopic and Electrochemical Properties. [Fe(BLPA)DBC]BPh_4 is an air-sensitive purple-blue complex. The visible spectrum of BLPA complex is dominated by two intense bands at 583 and 962 nm in CH_3CN under argon (ε = 2600 and 4400 $M^{-1}cm^{-1}$, respectively). These bands are assigned to the catecholate to Fe(III) charge transfer bands based on the extinction coefficient, spectral shifts with various substituted catechols, and the comparison with known [Fe^{III}(L)DBC] complexes. But it has stronger intensities than those of previous [Fe^{III}(L)DBC] complexes (ε = 1200-2500 $M^{-1}cm^{-1}$).[12-16] Furthermore, these values are the most red-shifted of the [Fe^{III}(L)DBC] series (Table 1). The lowest energies of these transitions clearly demonstrate that the Fe(III) center in the BLPA complex has the most Lewis acidity among the series of [Fe(L)DBC] complexes. This is not a surprising result since the BLPA ligand provides all neutral nitrogen donors and weak binding to metal center due to the steric effect of the 6-methyl substituents on the pyridine rings. It is well established that ligands with 6-methyl substituents favor a metal center with a larger ionic radius, *i.e.*, high-spin over low-spin complex due to the steric effect.[22]

Table 1. Comparison of the Properties of the [Fe(L)DBC] Complexes

	PDA[a]	BPG[a]	TPA[b]	BLPA
λ_{max} (nm) in CH_3CN	444, 688	488, 764	568, 803	583, 962
E^o (DBC/DBSQ)(mV)[c]	255	342	500	521
intradiol cleavage yield	95%	97%	98%	75%
extradiol cleavage yield	0%	0%	0%	15%
k_{O2} in CH_3OH (10^{-2} M^{-1} s^{-1})[d]	5.0	43	1000	72
k_{O2} in DMF (10^{-2} M^{-1} s^{-1})[d]	4.3	18	1500	9
δ (5-*t*-and 3-*t*-Bu)(ppm)[e]	5.1, 1.6	6.4, 4.6	8.7, 5.2	10.0, 6.5
δ (DBC 6- and 4-H) (ppm)	16, 9	8, −18	−5, −57	1.8, −84
δ (pyridine β-H) (ppm)	97, 81	95, 86	92, 90	86, 84

[a] Reference 14. [b] Reference 15. [c] Potential are referenced *vs.* SCE and obtained in DMF with 0.1 M $TBABF_4$ as supporting electrolyte. [d] $k_{O2}=k_{obs}/[O_2]$. [e] Measured in CD_3CN.

The electrochemistry of the BLPA complex shows a quasi-reversible redox couple of DBC/DBSQ at 521 mV *vs.* SCE in DMF, which is considerably more positive than the free DBC/DBSQ couple (Figure 1).[23] This large positive shift indicates that the coordination of the DBC to the ferric center significantly stabilizes the DBC oxidation state. The potentials observed also reflect the Lewis acidity of metal center as modulated by the tetradentate ligand. Complex of the less basic ligands exhibits more positive DBC/DBSQ potentials, indicating a greater stabilization of the DBC oxidation state by the more Lewis acidic iron center (Table 1). Therefore, the BLPA complex has the most Lewis acidic iron(III) center among [Fe^{III}(L)DBC] complexes.

NMR Properties. The [Fe^{III}(L)DBC] complexes exhibit large NMR contact shifts, which provide some information regarding the electronic structure of the com-

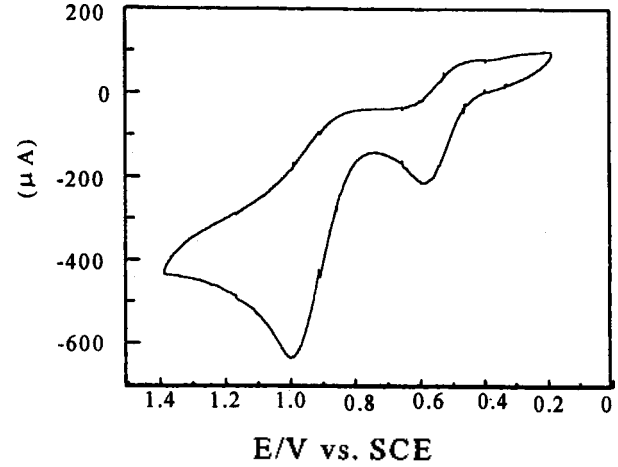

Figure 1. Cyclic voltammogram of [Fe(BLPA)DBC]BPh_4 in CH_3CN under argon with 0.1 M $TBABF_4$ as supporting electrolyte. Potential is referenced *vs.* SCE with no correction for junction potentials. The wave at 990 mV corresponds to the oxidation of BPh_4 counter anion.

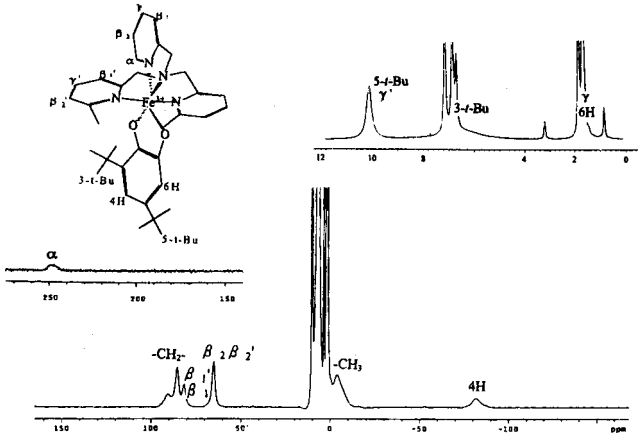

Figure 2. ^{1}H NMR spectrum of [Fe(BLPA)DBC]BPh_4 in CD_3CN under argon with ambient conditions. The right inset is an expansion of diamagnetic region of the main spectrum. The two peaks at 7.3 and 6.9 ppm correspond to the protons of BPh_4 counter anion.

plexes.[14,15] The NMR spectrum of BLPA complex is dominated by the picolyl and lutidyl beta protons, which appear as relatively sharp features at 86 and 84, and 66 ppm with T_1 values of 1.8 and 2.0, and 1.3 ms, respectively (Figure 2).[24] The picolyl beta proton peak is similar to that of [Fe^{III}(TPA)DBC] complex (90 ppm).[15] The picolyl alpha protons are broadened due to their proximity to the metal center and shifted further downfield at 249 ppm, whereas the methyl protons of lutidyl appear as broad peak at −3.9 ppm with T_1 value of 0.3 ms. The gamma protons of picolyl and lutidyl resonate in the diamagnetic region at 8.1 ppm and 1.7 ppm, which can be obscured by other features. Additional peaks arise from the methylene protons, which appear as broad bands at 92 ppm for picolyl and 86 ppm for lutidyl with T_1 value of 1.0 and 1.7 ms. The DBC-5-*t*-butyl and 3-*t*-butyl proton resonances are found at 10.0 and 6.5 ppm with T_1 values of 6.85 and 1.78 ms, respectively. The obscure peaks are confirmed by using the various delay times (d_1) of inversion-recovery (T_1) pulse in order to remove the diamagnetic signals. The DBC 6-H and 4-H protons for BLPA complex exhibit shifts at 1.8 and −84 ppm in CD_3CN, respectively. The assignments can be confirmed by the ^{1}H NMR spectrum of the selectively deuterated [Fe(BLPA)(DBC-4,6-d_2)]BPh_4 complex. The less upfield shifted resonance is the broader of the two protons and thus assigned to 6-H proton due to its proximity to the metal center.

Very strikingly, the catecholate shifts exhibit a remarkable dependence on the nature of the tetradentate ligands (Table 1). The DBC 6-H and 4-H proton resonances go from being downfield shifted for the PDA complexe to being upfield shifted for the TPA complex, and further upfield shifted for the BLPA complex. Futhermore, the variable temperature ^{1}H NMR study shows that the DBC 6-H and 4-H proton resonances are not changed from upfield shifted to diamagnetic region as the temperature is increased (Figure 3). Thus, we attribute the large variation in the DBC shifts to an increased semiquinone character due to the enhanced covalency of the metal-catecholate interaction as the series progresses from PDA to BLPA complex. On

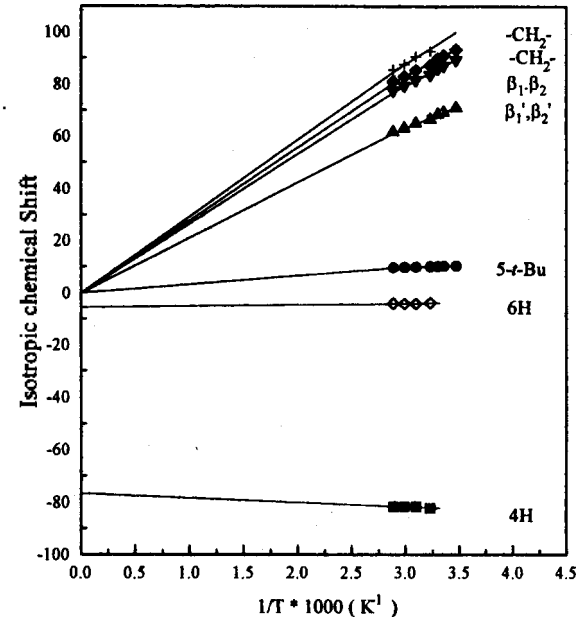

Figure 3. Plot of chemical shift (δ) *vs.* 1/Temp. (1/K) of [Fe(BLPA)DBC]BPh_4 in CD_3CN under argon.

the other hand, the tripodal ligand shifts as monitored by the picolyl β-H's remain in the same downfield region for the entire series (Table 1). The beta protons of lutidine bound to high spin Fe^{III} centers such as [Fe(BLPA)Cl_2]$^+$ are found at ~70 ppm.[25] Based on these comparisons, all the pi-

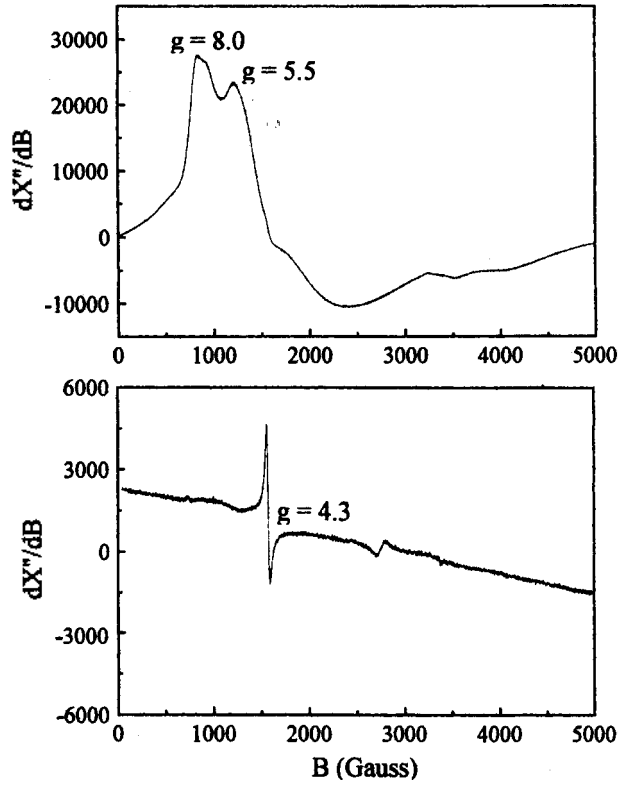

Figure 4. X-band EPR spectra: (a) [Fe(BLPA)DBC]BPh_4 in CH_3CN under argon. (b) [Fe(BLPA)DBC]BPh_4 in CH_3CN after the oxygenation. Spectra were obtained at 9.22 GHz with 100 kHz modulation at 4 K.

colyl β-H shifts in the [Fe^{III}(L)DBC] series are indicative of high spin Fe^{III}, which are consistent with other spectroscopic data. Indeed, EPR spectrum of the BLPA complex exhibits g=5.5 and 8.0 at 4 K, which are typical values of axially symmetric high-spin Fe^{III} complexes, with no indication of semiquinone radical signals (Figure 4a). Thus, the semiquinone character is too small to be manifested in the structural data. It also does not affect the pyridine isotropic shifts significantly because the isotropic shifts due to high spin ferric and ferrous centers are comparable in magnitude. The semiquinone character is manifested in the DBC shifts because of the large differences in unpaired spin density expected for a catecholate coordinated to a paramagnetic center versus a semiquinone. A coordinated catecholate would gain unpaired spin density *via* spin delocalization from the paramagnetic center, while a semiquinone is itself a paramagnetic center. The shift patterns for the various DBC protons are consistent with an increasing semiquinone character from the PDA to the BLPA complex.

EPR studies and MO calculations[26] on semiquinones have demonstrated substantial unpaired spin density at C-4 and C-5 and significantly smaller density at C-3 and C-6. Thus, the 5-*t*-butyl exhibits a larger downfield shift relative to the 3-*t*-butyl group and the 4-H proton is significantly more upfield shifted than the 6-H proton. In the BLPA complex, these effects are even more pronounced when compared to other complexes. The greater semiquinone character in the BLPA complex correlates well with its high reactivity towards O_2.

Reactivity and Kinetics. The [Fe^{III}(L)DBC] complexes all react with dioxygen to yield products due to the oxidative cleavage of the catechol ring.[14,15] The BLPA complex reacts with O_2 within a few hours to afford intradiol and extradiol cleavage products resulting from C-C oxidative cleavage of the catechol ring. The products isolated from the reaction mixture are intradiol cleavage products; 3,5-di-*tert*-butyl-1-oxacyclohepta-3,5-diene-2,7-dione (45%), 3,5-di-*tert*-butyl-5-(carboxymethyl)-2-furanone (30%) and extradiol cleavage products; 3,5-di-*tert*-butyl-2-pyrone 5%, 4,6-di-*tert*-butyl-2-pyrone (10%), 3,5-di-*tert*-butyl-5-(formyl)-2-furanone (trace amount). This is the first time to obtain both intradiol and extradiol cleavage products for the [Fe^{III}(L)DBC] complexes. Even though Dei *et al.* reported that the extradiol products (35% yield) can be obtained for [Fe^{III}(TACN)DBC]$^+$ complex, they did not get an intradiol cleavage product at all.[27] Que *et al.* also reported very recently that the extradiol products (quantitative yield) can be obtained for [Fe^{III}(TACN)DBC(Cl)] complex by adding excess amount of bases.[28]

As earlier observed,[14,15] the anhydride (3,5-di-*tert*-butyl-1-oxacyclohepta-3,5-diene-2,7-dione) is the major product of intradiol cleavage. However, the Fe^{III} center in BLPA complex appears to promote hydrolysis of the anhydride to muconic acid and subsequent ring closure to form the furanone acid (3,5-di-*tert*-butyl-5-(carboxymethyl)-2-furanone). This conversion results in the assembly of an (μ-oxo)diiron(III) BLPA complex with the furanone acid bridging the two metal centers, with UV-Vis and NMR spectral properties very similar to those of the [Fe^{III}_2O(BLPA)$_2$(O_2CCH$_3$)](ClO$_4$)$_3$ complex obtained by direct synthesis. Furthermore, EPR

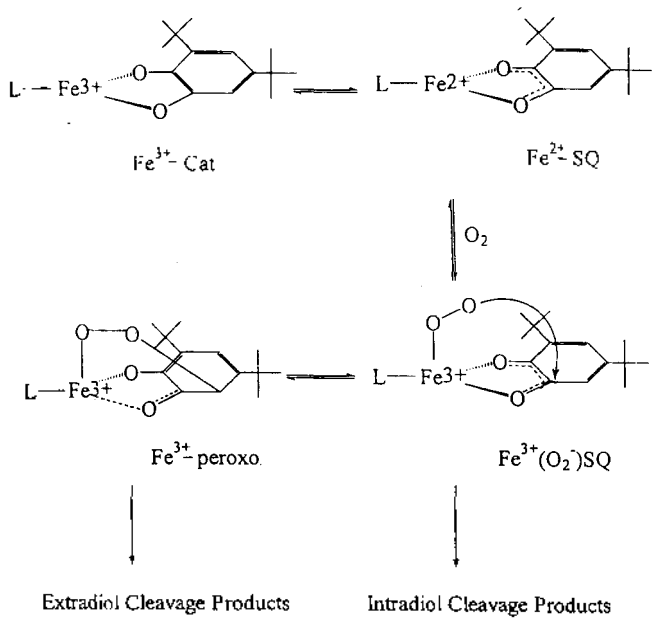

Scheme 2.

spectrum of the BLPA complex after oxygenation shows almost no EPR signal except very small amount of Fe^{III} complex, indicating the iron(III) centers are antiferromagnetically coupled (Figure 4b).

In addition, extradiol cleavage products might be originated from the byproduct during the reaction process of peroxy radical attack to catechol ring (substrate activation mechanism) or the decomposition of Fe^{III}-DBSQ-peroxide as a result of Fe^{III}-superoxide species attacking to catechol ring (oxygen activation mechanism)[28] (Scheme 2). This ob-

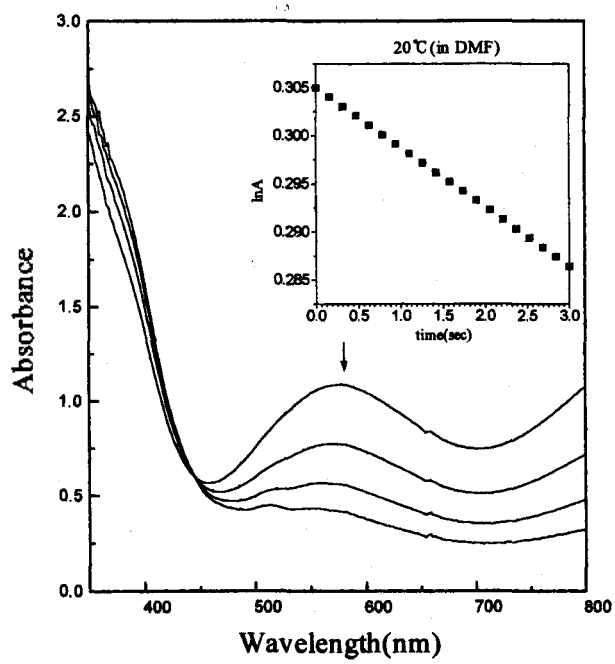

Figure 5. Oxygenation process of the reaction of [Fe(BLPA)DBC]BPh$_4$ in DMF with O_2 as monitored by disappearance of catecholate to Fe^{III} charge transfer bands. Inset: Plot of ln A *vs.* time for the [Fe(BLPA)DBC]BPh$_4$ reaction at 20 °C.

servation is consistent with the trend earlier noted that the yield of intradiol cleavage products increases as the Lewis acidity of the metal center increases.[14]

Kinetic studies of the reaction of the complex with 1 atm O_2 in CH_3OH under pseudo-first order conditions show that the BLPA complex reacts quite faster than the PDA complex (Figure 5). But it reacts much slower than the corresponding TPA complex due to the steric effect of methyl substituent on the pyridyl ring (Table 1). This result represents that the steric effect is also a crucial factor for determining the oxygenation rate. Based on the earlier arguments, both the high specificity and the fast kinetics can be associated with the high Lewis acidity of the ferric center in the BLPA complex, but needed to consider the steric effect.

These results provide substantial support for the substrate activation mechanism proposed for the oxidative cleavage of catechols,[18] in which O_2 attack on the coordinated catecholate is facilitated by the enhanced radical character of the substrate (Scheme 1). A peroxide complex is proposed to form subsequent to O_2 binding and then decompose to the muconic anhydride. The recently reported crystal structure of the O_2 adduct of an Ir(III)-catecholate complex shows just such a peroxide moiety coordinated in a tridentate manner to the Ir center,[29] a result that lends further credence to the mechanism shown in Scheme 1. However, when we introduce the hydrophobic pocket (*e.g.*, methyl substituent) around the metal center as in real enzyme system, the substituent does interfere in the oxygenation pathway and thus reduce the specificity of the intradiol cleavage products, but give rise to some extradiol cleavage products. Therefore, we might need to consider the steric effect as well as the electronic effect toward understanding the oxygenation process of catechol dioxygenases.

Acknowledgment. This work has been supported by Advanced Materials Chemistry Research Center at Korea university and the Korea Science and Engineering Foundation (Grant No. 951-0303-008-2).

References

1. For recent reviews of these enzymes, see: (a) Que, L., Jr. *Adv. Inorg. Biochem.* **1983**, *5*, 167. (b) Dekkar, M. in Microbial Degradation of Organic Molecules: Gibson, D. T. Ed.; New York, 1984, 535. (c) Que, L., Jr. *J. Chem. Educ.* **1985**, *62*, 938. (d) Que, L., Jr. in Iron Carriers and Iron Proteins; Loehr, T. M., Ed.; VCH Publishers: New York, 1989, 467. (e) Que, L., Jr. and Ho, R. Y. N. in Dioxygen Activation by Enzymes with Mononuclear Iron Active Sites, *Chem. Rev.* **1996**, *96*, 2607-2624.
2. Kent, T. A.; Münck, E.; Pyrz, J. W.; Widom, J.; Que, L., Jr. *Inorg. Chem.* **1987**, *26*, 1402.
3. (a) Que, L., Jr.; Heistand, R. H., II; Mayer, R.; Roe, A. L. *Biochemistry* **1980**, *19*, 2588. (b) Que, L., Jr.; Epstein. R. M. *Biochemistry* **1981**, *20*, 2545.
4. Whittaker, J. W.; Lipscomb, J. D. *J. Biol. Chem.* **1984**, *259*, 4487.
5. Felton, R. H.; Barrow, W. L.; May, S. W.; Sowell, A. L.; Goel, S. *J. Am. Chem. Soc.* **1982**, *104*, 6132.
6. Que, L., Jr.; Lauffer, R. B.; Lynch, J. B.; Murch, B. P.; Pyrz, J. W. *J. Am. Chem. Soc.* **1987**, *109*, 5381.
7. (a) Bull, C.; Ballou, D. P.; Otsuka, S. *J. Biol. Chem.* **1981**, *256*, 12681. (b) Walsh, T. A.; Ballou, D. P.; Mayer, R.; Que, L., Jr. *J. Biol. Chem.* **1983**, *258*, 14422.
8. (a) Ohlendorf, D. H.; Lipscomb, J. D.; Weber, P. C. *Nature* **1988**, *336*, 403. (b) Ohlendorf, D. H.; Orville, A. M.; Lipscomb, J. D. *J. Mol. Biol.* **1994**, *244*, 586.
9. (a) Whittaker, J. W.; Lipscomb, J. D.; Kent, T. A.; Munck, E.; Orme-Johnson, N. R.; Orme-Johnson, W. H. *J. Biol. Chem.* **1984**, *259*, 4466. (b) Orville, A. M.; Lipscomb, J. D. *J. Biol. Chem.* **1989**, *264*, 8791. (c) True, A. E.; Orville, A. M.; Pearce, L. L.; Lipscomb, J. D.; Que, L., Jr. *Biochemistry* **1990**, *29*, 10847.
10. Orville, A. M.; Ohlendorf, D. H.; Lipscomb, J. D. unpublished results.
11. (a) Funabiki, T.; Tada, S.; Yoshioka, T.; Takano, M.; Yoshida, S. *J. Chem. Soc., Chem. Commun.* **1986**, 1699. (b) Funabiki, T.; Mizoguchi, A.; Sugimoto, T.; Tada, S.; Tsuji, M.; Yoshioka, T.; Sakamoto, H.; Takano, M.; Yoshida, S. *J. Am. Chem. Soc.* **1986**, *108*, 2921. (c) Funabiki, T.; Konishi, T.; Kobayashi, S.; Mizoguchi, A.; T. M.; Takano, M.; Yoshida, S. *Chem. Lett.* **1987**, 719.
12. Que, L., Jr.; Kolanczyk, R. C.; White, L. S. *J. Am. Chem. Soc.* **1987**, *109*, 5373.
13. Cox, D. D.; Benkovic, S. J.; Bloom L. M.; Bradley, F. C.; Nelson, M. J.; Que, L., Jr.; Wallick, D. E. *J. Am. Chem. Soc.* **1988**, *110*, 2026.
14. Cox, D. D.; Que, L., Jr. *J. Am. Chem. Soc.* **1988**, *110*, 8085.
15. Jang, H. G.; Cox, D. D.; Que, L., Jr. *J. Am. Chem. Soc.* **1991**, *113*, 9200.
16. Koch, W. O.; Krüger, H.-J. *Angew. Chem. Int. Ed. Engl.* **1995**, *34*, 2671.
17. Abbreviations: PDA, N-carboxymethyl-N-(2-pyridylmethyl)glycine; BPG, N,N-bis(2-pyridyl-methyl)glycine; TPA, tris(2-pyridylmethyl)amine; DBCH2, 3,5-di-*tert*-butylcatechol; TACN, triazacyclononane; BPLA is bis(2-pyridylmethyl)(6-methyl-2-pyridylmethyl)amine.
18. Que, L., Jr.; Lipscomb, J. D.; M nck, E.; Wood, J. M. *Biochim. Biophys. Acta* **1977**, *485*, 60.
19. Pyrz, J. W.; Roe, A. L.; Stern, L. J.; Que, L., Jr. *J. Am. Chem. Soc.* **1985**, *107*, 614.
20. de Mota, M. M.; Rodgers, J.; Nelson, S. N. *J. Chem. Soc.* (A), **1969**, 2036.
21. (a) Norman, R. E.; Yan, S.; Que, L., Jr.; Backes, G.; Ling, J.; Sander-Loehr, J.; Zhang, J. H.; O'Connor, C. J. *J. Am. Chem. Soc.* **1990**, *112*, 1554. (b) Norman, R. E.; Holz, R. C.; Menage, S.; O'Connor, C. J.; Zhang, J. H.; Que, L., Jr. *Inorg. Chem.* **1990**, *29*, 4629.
22. Zang, Y., Kim, J.; Dong, Y.; Wilkinson, E. C.; Appelman, E. H.; Que, L., Jr. *J. Am. Chem. Soc.* **1997**, *119*, 4197.
23. Nanni, E. J., Jr.; Stallings, M. D.; Sawyers, D. T. *J. Am. Chem. Soc.* **1980**, *102*, 4481.
24. All peak assignments were based on the T_1 values and integrations, and by comparison with the spectra of the $[Fe(BLPA)Cl_2]Cl$, $[Fe(TPA)DBC]BPh_4$, and [Fe(BLPA) DBC]BPh_4 complex.
25. Lim, J. H.; Jang, H. G. unpublished results.
26. (a) Kahn, O.; Prins, R.; Reedijk, J.; Thompson, J. S. *Inorg. Chem.* **1987**, *26*, 3557. (b)Yamabe, S.; Minato,

T.; Kimura, M. *J. Phys. Chem.* **1981**, *85*, 3510. (c) Trapp, C.; Tyson, C. A.; Giacometti, G. *J. Am. Chem. Soc.* **1968**, *90*, 1394.
27. Dei, A.; Gatteschi, D.; Pardi, L. *Inorg. Chem.* **1993**, *32*, 1389.
28. Ito, M.; Que, L., Jr. *Angew. Chem. Int. Ed. Engl.* **1997**, *36*, 1342.
29. (a) Barbaro, P.; Bianchini, C.; Mealli, C.; Meli, A. *J. Am. Chem. Soc.* **1991**, *113*, 3181. (b) Barbaro, P.; Bianchini, C.; Linn, K.; Mealli, C.; Vizza, F.; Laschi, F.; Zanello, P. *Inorg. Chim. Acta* **1992**, *198-200*, 31.

Determination of Isotopic Ratios for Ca in Inductively Coupled Plasma Mass Spectrometry (ICPMS) by Removing Water Related Molecules

Yong-Nam Pak* and S. R. Koirtyohann†

**Department of Chemistry, Korea National University of Education, Cheong Won 363-791, Korea*
†Department of Chemistry, University of Missouri, Columbia, MO 65201, U. S. A.
Received July 19, 1997

Calcium isotopic ratios are precisely measured by removing isobaric interferences originated from water in the plasma. Liquid Ar cryogenic trap combined with membrane desolvator could eliminate backgrounds at m/z 42 and 44. Slow drift of ICP-MS is corrected by the frequent running of the standards. It is found necessary to separate Ca from the sample matrix using Ca oxalate precipitation technique. Currently, the RSD is 0.5-1.0% for 2 minutes of measurement but is expected to be improved if the measurement time is increased. The technique was applied to ^{42}Ca enriched baby fecal samples and successfully determined ^{42}Ca/^{44}Ca ratio changes.

Introduction

Since the development of ICP-MS,[1] it has been established well in the elemental analysis and isotopic ratio measurement of most elements.[2-3] Stable isotopes have been used as tracers to monitor isotopic variations in biology[4] and environmental studies.[5] However, because of large backgrounds from Ar related species, certain elements such as Fe, Ca, and K could not be measured easily. Several different approaches[6-12] have been made to reduce the background in the mass range of 39-57 and measure the isotopic ratios of these important elements precisely.

Taylor *et al.*[6] used an air-acetylene flame as an ion source to determine isotopic ratios for K with a quadrupole mass spectrometer. The detection limit was 2-3 ppb and the ratio of ^{41}K/^{39}/K was measured with 0.5-1% relative standard deviation (RSD). Different ion sources such as helium[7] or nitrogen[8] plasma were also used. However, Helium or Nitrogen plasma/MS technique requires an additional instrument or a large modification such as adding an additional vacuum pump because helium is not easily pumped out. Furthermore, it is not easy to change the plasma source from Ar to another. Some scientists[9,10] attempted to use the scavenger gases such as CH^4 and Xe to the plasma or carrier gas to suppress the ^{40}ArO background for the determination of Fe. Jiang *et al.*[11] used a relatively cool plasma to reduce ArH and was able to alleviate interferences for determination of K isotopes. Park[12] was recently able to reduce molecular backgrounds in the mass range of 39-57 successfully. He used a cool plasma condition and a copper shield to reduce the secondary discharge at the interface. Isotopic ratios of K, Ca, Cr and Fe could be measured precisely but the mass discrimination against low mass was severe. Furthermore, both authors[11,12] mentioned that it might not be possible for a certain ICPMS to reduce the background by using the "cooled" plasma condition. Indeed it was not possible to reduce the background enough to measure the precise isotopic ratio with the model used (Elan 5000) in this research by using the "cooled" condition.

The method developed in this experiment is to use a cryogenic cooling system to remove background produced from water. It does not require any expensive additional apparatus but effectively removes background molecules such as ArO, ArOH and ArH. The elimination of water will greatly alleviate background overlaps because these molecules are mostly produced from the reaction between water and Ar. In the earlier report,[13] it was shown that isotope of Fe, Cu, Li, and Zn could be measured precisely (0.1%) with this technique. In this report, this technique is applied to the measurement of Ca isotope ratio.

Ca is an important biological and environmental element. It has been used in human bodies as a stable isotope tracer? because it is safe compared to radio tracers.[4] The minimal tracer is added because of the high cost of isotope enriched material. Only small dose of stable isotopic tracer is added and its isotopic perturbation should be measured precisely. Ca has several isotopes (mass number 40, 42, 43, 44, 46, 48) and their backgrounds are interfered with ArH_2 (42), CO_2 and N_2O(44), NOH_2O(46) and ArC(48). With cryogenic cooling, backgrounds at 42 and 44 could be sub-

*To whom correspondence should be sent.